

Synthesis and photochemical study of a supramolecular pseudodimeric complex of 4-styrylpyridinium derivatives*

E. N. Ushakov,^{a,b} A. I. Vedernikov,^b S. K. Sazonov,^b L. G. Kuz'mina,^c M. V. Alfimov,^b
J. A. K. Howard,^d and S. P. Gromov^{b*}*

^a*Institute of Problems of Chemical Physics, Russian Academy of Sciences,
1 prosp. Akad. Semenova, 142432 Chernogolovka, Moscow Region, Russian Federation.*

Fax: +7 (496) 522 3507. E-mail: en-ushakov@mail.ru

^b*Photochemistry Center, Russian Academy of Sciences,
7A-1 ul. Novatorov, 119421 Moscow, Russian Federation.*

Fax: +7 (495) 936 1255. E-mail: spgromov@mail.ru

^c*N. S. Kurnakov Institute of General and Inorganic Chemistry, Russian Academy of Sciences,
31 Leninsky prosp., 119991 Moscow, Russian Federation.*

Fax: +7 (495) 954 1279

^d*Department of Chemistry, Durham University,
South Road, Durham DH1 3LE, UK*

1-(3-Ammoniopropyl)-4-[(*E*)-2-(3,4-dichlorophenyl)vinyl]pyridinium diperchlorate was synthesized and its crystal structure was studied by X-ray diffraction. The photochemical properties of this compound and its complexation with a 18-crown-6-containing derivative of 4-styrylpyridine were studied by electronic spectroscopy. These compounds form a supramolecular complex ($\log K = 3.89$ in MeCN at an ionic strength of 0.01 mol L^{-1}), in which the styryl chromophores are arranged one above another due to stacking interactions. The complexation activates the cross [2+2] photocycloaddition of styrylpyridine derivatives. A procedure is proposed for the global analysis of spectrophotometric data, which takes into account the effect of the ionic strength of the solution on the observed equilibrium reaction.

Key words: 4-styrylpyridinium salts, *E*–*Z*-photoisomerization, fluorescence, pseudodimeric complex, stability constant, supramolecular [2+2] photocycloaddition.

The development and improvement of methods for controlling chemical and photochemical reactions is an important area of research in supramolecular chemistry. The molecular self-assembly *via* non-covalent interactions is efficiently used to control photoreactions both in homogeneous solutions^{1–5} and in the solid state.^{4–7} The self-assembly through hydrogen bonding is of particular interest; however, examples of its application to photosensitive compounds in homogeneous solutions are scarce.

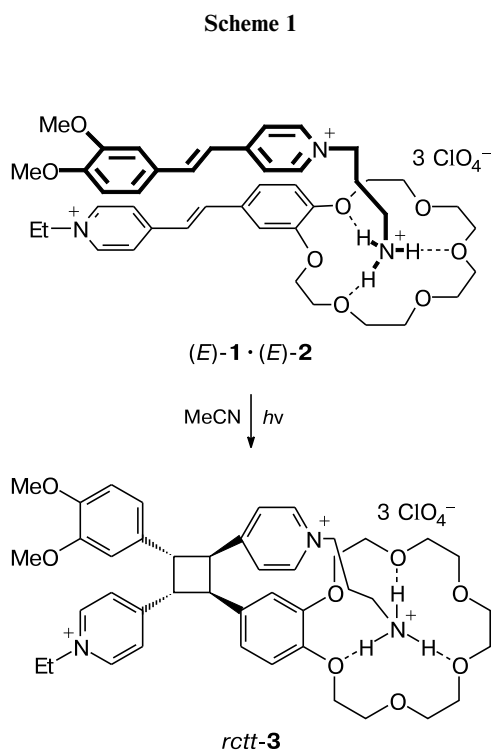
The [2+2] photocycloaddition (PCA) of unsaturated compounds is a classical photoreaction commonly employed in organic synthesis. In solution, intermolecular [2+2] PCA reactions are usually characterized by very low quantum yields because of a short lifetime of the electronic excited state and afford mixtures of isomeric cyclobutanes. One of the first examples of the molecular self-assembly, which initiates the stereospecific [2+2] PCA in homogeneous solutions, is the preparation of pseudocyclic

dimeric complexes of the betaine-type crown-containing styryl dye with Mg^{2+} ions that are formed *via* double ion pairing.^{8,9} Later, highly stable pseudocyclic complexes of unsaturated compounds were characterized, in which the molecules are held together by double or quadruple intermolecular cation–macrocycle interactions involving hydrogen bonds between the primary or secondary ammonium group and the complementary crown moiety.^{10–14} This self-assembly approach was used to perform the stereoselective photochemical synthesis of cyclobutanes from crown-containing derivatives of stilbene¹⁴ and 4-styrylpyridine.¹³

The self-assembly *via* a single cation–macrocycle interaction involving hydrogen bonds between the primary ammonium group and the 18-crown-6 moiety was applied to control cross [2+2] PCA reactions.^{15,16} Scheme 1 shows the stereospecific photoreaction between styryl dyes, one of which contains the 18-crown-6 moiety (compound (*E*)-1), whereas another dye contains the ammoniopropyl group (compound (*E*)-2). It was found¹⁵ that compounds (*E*)-1 and (*E*)-2 in MeCN, taken at concentrations of

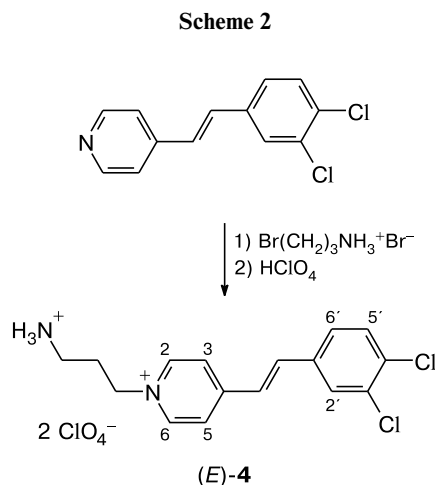
* Dedicated to Academician of the Russian Academy of Sciences V. I. Minkin on the occasion of his 80th birthday.

$\sim 10^{-3}$ mol L $^{-1}$, form the pseudodimeric complex (*E*)-**1**·(*E*)-**2**, in which the styrylpyridinium cations are arranged one above another due to stacking interactions (in polar solvents, these interactions are stronger than the Coulomb repulsion between the cations). In the complex (*E*)-**1**·(*E*)-**2**, the dye molecules are subjected to two competing reactions, *viz.*, the *E*–*Z*-photoisomerization and cross [2+2] PCA, the latter occurring stereospecifically to give cyclobutane **3** as the only *rc**tt*-isomer. Since photoinduced *Z*-isomers of dyes **1** and **2** are not involved in PCA, cyclobutane *rc**tt*-**3** can be selectively prepared, under particular photolysis conditions, in high yield.



We suggested that pseudodimeric complexes of styryl dyes can be used as a convenient model for the investigation of the role of electronic factors in cross [2+2] PCA. The measurements of the stability constants of pseudodimeric complexes and the quantum yields of the supramolecular photoreaction require the development of simple and reliable spectrophotometric procedures. It should be noted that it is virtually impossible to measure the stability constant of the complex (*E*)-**1**·(*E*)-**2** by spectrophotometric titration of receptor (*E*)-**1** with substrate (*E*)-**2** because these reagents have similar absorption spectra. Another distinguishing feature of the complexation of cation (*E*)-**1** with dication (*E*)-**2** is the dependence of the stability constant on the ionic strength of the solution. In order to test different spectrophotometric procedures, we synthesized a dichloro-substituted analog of dye (*E*)-**2** (compound (*E*)-**4**, Scheme 2), the absorption spectrum of which

is hypsochromically shifted with respect to compounds (*E*)-**1** and (*E*)-**2**. The structure of compound (*E*)-**4** was established by X-ray diffraction.



In the present study, we report on the results of investigation of the photochemical properties and complexation of (*E*)-**1** and (*E*)-**4** and propose a procedure for the global analysis of the spectrophotometric data, which takes into account the effect of the ionic strength of the solution on the complexation. The structure of the pseudodimeric complex (*E*)-**1**·(*E*)-**4** was studied by quantum chemical modeling.

Experimental

Instrumentation. The melting points (uncorrected) were measured in capillaries on a Mel-Temp II instrument. The elemental analysis was carried out in the Laboratory of Microanalysis of the A. N. Nesmeyanov Institute of Organoelement Compounds of the Russian Academy of Sciences (Moscow).

The ^1H and ^{13}C NMR spectra were recorded on a Bruker DRX500 spectrometer (500.13 and 125.76 MHz, respectively) in DMSO- d_6 using the signal of the solvent as the internal standard (δ_{H} 2.50, δ_{C} 39.43). The chemical shifts and the spin-spin coupling constants were measured with an accuracy of 0.01 ppm and 0.1 Hz, respectively. The assignment of the signals for protons and carbon atoms was made based on two-dimensional heteronuclear correlation spectra (HSQC and HMBC). The 2D experiments were performed using standard parameters included in the Bruker software. The HMBC experiment was optimized for the constant $J_{\text{H,C}} = 8$ Hz.

The electronic absorption spectra were recorded on a Specord M40 (Carl Zeiss Jena) spectrophotometer in quartz cuvettes with ground-in stoppers and the optical path length $l = 10, 2, 1,$ and 0.5 mm.

The stationary fluorescence spectra were measured on a PerkinElmer LS 55 spectrofluorometer at a constant photodetector voltage. The corrected spectra were recorded taking into account the spectral sensitivity curve for the photodetector indicated by the provider. The fluorescence lifetimes were determined on a PicoQuant FluoTime 200 spectrometer. A semi-

conductor pulsed laser ($\lambda = 375$ nm, pulse duration ~ 75 ps) was used as an excitation source.

The stationary photolysis was performed with light from a DRS-250 high-pressure mercury lamp. The 313 or 366 nm mercury lines were isolated using colored optical glass filters. The light intensity at $\lambda = 366$ nm was measured using a PP-1 cavity receiver.

Materials. 3-Bromo-1-propylammonium bromide, 70% perchloric acid (Aldrich), and MeCN (Kriokhrom, special purity grade, water content < 0.03 vol.%) were used without additional purification. Tetrabutylammonium perchlorate (Fluka, $\geq 99.0\%$) and anthracene (analytical grade) were purified by recrystallization from ethanol. Propane-1,3-diammonium diperchlorate, 4-[(*E*)-2-(2,3,5,6,8,9,11,12,14,15-decahydro-1,4,7,10,13,16-benzohexaoxacyclooctadecin-18-yl)vinyl]-1-ethylpyridinium perchlorate (compound (*E*)-1), and 4-[(*E*)-2-(3,4-dichlorophenyl)vinyl]pyridine were synthesized according to known procedures.^{17–19}

1-(3-Ammoniopropyl)-4-[(*E*)-2-(3,4-dichlorophenyl)vinyl]pyridinium diperchlorate ((*E*)-4). A mixture of 4-[(*E*)-2-(3,4-dichlorophenyl)vinyl]pyridine (0.30 g, 1.20 mmol) and 3-bromo-1-propylammonium bromide (1.43 g, 6.53 mmol) was heated for 6 h in the dark at 160 °C (oil bath). After cooling, the reaction mixture was triturated with hot 96% ethanol (8 mL) and cooled to 5 °C. The precipitate was filtered off, washed with cold ethanol (2×3 mL), and dried in air. Crude 1-(3-ammoniopropyl)-4-[(*E*)-2-(3,4-dichlorophenyl)vinyl]pyridinium dibromide was obtained as a pale-beige powder in a yield of 0.42 g (75%, 0.90 mmol). The precipitate was dissolved with heating in a mixture of 96% ethanol (15 mL) and distilled water (1 mL). Then 70% perchloric acid (0.38 mL, 4.40 mmol) was added, and the mixture was cooled to 5 °C. The crystalline precipitate that formed was filtered off, washed with 96% ethanol (2 mL), and dried in air. Compound (*E*)-4 was obtained in a yield of 0.35 g (57%) as a nearly colorless finely crystalline powder, m.p. 257–258 °C (with decomp., from ethanol). Found (%): C, 37.69; H, 3.38; N, 5.45. $C_{16}H_{18}Cl_4N_2O_8$. Calculated (%): C, 37.82; H, 3.57; N, 5.51. 1H NMR (25 °C), δ : 2.23 (m, 2 H, $CH_2CH_2NH_3$); 2.87 (m, 2 H, CH_2NH_3); 4.64 (t, 2 H, CH_2N , $^3J = 7.0$ Hz); 7.70 (d, 1 H, $CH=CHPy$, $^3J = 16.4$ Hz); 7.74 (dd, 1 H, H(6'), $^3J = 8.2$ Hz, $^4J = 2.3$ Hz); 7.79 (d, 1 H, H(5'), $^3J = 8.2$ Hz); 7.89 (br.s, 3 H, NH_3^+); 8.05 (d, 1 H, $CH=CHPy$, $^3J = 16.4$ Hz); 8.07 (d, 1 H, H(2'), $^4J = 2.3$ Hz); 8.29 (d, 2 H, H(3), H(5), $J = 6.8$ Hz); 9.05 (d, 2 H, H(2), H(6), $J = 6.8$ Hz). ^{13}C NMR (30 °C), δ : 28.40 ($CH_2CH_2NH_3$); 35.67 (CH_2NH_3); 56.93 (CH_2N); 124.26 (C(3), C(5)); 125.34 ($CH=CHPy$); 128.09 (C(6')); 129.30 (C(2')); 131.16 (C(5')); 131.83 (C(3')); 132.42 (C(4')); 135.82 (C(1')); 137.94 ($CH=CHPy$); 144.44 (C(2), C(6)); 152.41 (C(4)). UV (MeCN), λ_{max}/nm (ϵ): 346 (37000).

Complex (*E*)-1·(*E*)-4. A solution of a mixture of compounds (*E*)-1 (7.4 mg, 13.6 μ mol) and (*E*)-4 (6.9 mg, 13.6 μ mol) in MeCN (3 mL) was slowly saturated with benzene vapor in the dark at ~ 20 °C (~ 2 weeks). The amorphous precipitate that formed was decanted and dried in air. The complex (*E*)-1·(*E*)-4 was obtained in a yield of 12.9 mg (90%) as a yellow powder, m.p. 154–157 °C. Found (%): C, 46.85; H, 5.00; N, 3.98. $C_{25}H_{34}ClNO_{10} \cdot C_{16}H_{18}Cl_4N_2O_8$. Calculated (%): C, 46.80; H, 4.98; N, 3.99.

X-ray diffraction study. Crystals of compound (*E*)-4 and propane-1,3-diammonium diperchlorate were grown by slow saturation of their solutions in MeCN with benzene vapor in the dark at ~ 20 °C.

Single crystals were mounted on a Bruker SMART-CCD diffractometer under a cold nitrogen stream ($T = 120(2)$ K). The crystallographic parameters and the intensities of experimental reflections were measured using Mo-K α radiation ($\lambda = 0.71073$ Å, graphite monochromator, ω -scan mode). The X-ray diffraction data were processed with the SAINT program²⁰ and were corrected for absorption using the SADABS program. The structures were solved by direct methods and refined by the full-matrix least-squares method based on F^2 with anisotropic displacement parameters for nonhydrogen atoms (except for the disordered atoms of the $Cl(2)O_4$ anion in structure 4, which were refined isotropically). The hydrogen atoms were positioned geometrically and refined isotropically (for $H_3N^+(CH_2)_3NH_3^+2ClO_4^-$) or using a riding model (for structure 4). The refinement of highly disordered structure 4 was performed using geometrical restraints (SADI, FLAT, ISOR).

All calculations were carried out with the SHELXTL-Plus program package.²¹ The crystallographic parameters and the X-ray diffraction data collection and refinement statistics are given in Table 1. The atomic coordinates and other experimental data were deposited in the Cambridge Crystallographic Data Centre (CCDC 1034272 (structure 4) and 1034273 ($H_3N^+(CH_2)_3NH_3^+ \cdot 2 ClO_4^-$)).

Electronic spectroscopy. Fluorescence quantum yields (ϕ_f) were determined using anthracene in ethanol as the reference ($\phi_f = 0.28$, see Ref. 22). The value of ϕ_f for the sample was calculated by the formula

$$\phi_f = (\phi_{fr} D_{ex} n^2 S) / (D_{ex} n_r^2 S_r),$$

where the subscript r refers to the parameters of the reference, D_{ex} is the optical density at the excitation wavelength of 330 nm ($D_{ex} < 0.05$), n is the refractive index of the solvent, and S is the integrated intensity of the corrected fluorescence spectrum in the scale of inverse centimeters.

The fluorescence lifetimes were determined by the global analysis of the decay curves measured at three different wavelengths. The general procedure for the global analysis of pulse spectroscopy data has been described earlier.²³

The quantum yields of the forward and reverse $E \rightarrow Z$ -photoisomerization reactions ($\phi_{E \rightarrow Z}$ and $\phi_{Z \rightarrow E}$, respectively) were determined from the kinetics of absorption spectra observed under stationary irradiation of a solution of the E isomer at $\lambda = 366$ nm. The concentrations of the isomers, $C_E(t)$ and $C_Z(t)$, were determined by the numerical solution of the kinetic equation

$$dC_E(t)/dt = 10^3 I_{act} [\phi_{Z \rightarrow E} \epsilon_Z C_Z(t) - \phi_{E \rightarrow Z} \epsilon_E C_E(t)] [1 - 10^{-D(t)}] / D(t),$$

$$D(t) = [\epsilon_E C_E(t) + \epsilon_Z C_Z(t)] l, \quad C_Z(t) = C_0 - C_E(t),$$

where I_{act} is the actinic light intensity ($\text{mol cm}^{-2} \text{s}^{-1}$), ϵ_E and ϵ_Z are the molar extinction coefficients of the isomers at the excitation wavelength ($\text{L mol}^{-1} \text{cm}^{-1}$), l is the cuvette length (cm), and C_0 is the concentration of the initial E isomer (mol L^{-1}). The absorption spectrum of the pure Z isomer was calculated from the spectra of the photostationary states reached under irradiation at different wavelengths (313 and 366 nm) on the assumption that the $\phi_{E \rightarrow Z} / \phi_{Z \rightarrow E}$ ratio is independent of the irradiation wavelength. All calculations were performed using the global analysis.²⁴

Table 1. Crystal parameters and the X-ray diffraction data collection and refinement statistics for compounds **4** and $\text{H}_3\text{N}^+(\text{CH}_2)_3\text{NH}_3^+ \cdot 2\text{ClO}_4^-$

Parameter	4	$\text{H}_3\text{N}^+(\text{CH}_2)_3\text{NH}_3^+ \cdot 2\text{ClO}_4^-$
Molecular formula	$\text{C}_{16}\text{H}_{18}\text{Cl}_4\text{N}_2\text{O}_8$	$\text{C}_3\text{H}_{12}\text{Cl}_2\text{N}_2\text{O}_8$
Molecular weight/g mol ⁻¹	508.12	275.05
Crystal system	Monoclinic	Monoclinic
Space group	$P2_1/c$	$P2_1/c$
<i>a</i> /Å	13.7468(13)	7.2512(2)
<i>b</i> /Å	15.9421(15)	14.3920(3)
<i>c</i> /Å	9.4227(9)	9.6503(2)
β/deg	98.566(3)	96.632(1)
<i>V</i> /Å ³	2042.0(3)	1000.36(4)
<i>Z</i>	4	4
<i>d</i> _{calc} /g cm ⁻³	1.653	1.826
<i>F</i> (000)	1040	568
μ(Mo- <i>K</i> α)/mm ⁻¹	0.628	0.679
Crystal dimensions/mm	0.26×0.10×0.04	0.54×0.14×0.05
Scan mode/θ-Scanning range/deg	ω/2.77–30.52	ω/2.55–29.00
<i>h, k, l</i> ranges	−19 ≤ <i>h</i> ≤ 19, −22 ≤ <i>k</i> ≤ 22, −13 ≤ <i>l</i> ≤ 10	−9 ≤ <i>h</i> ≤ 8, −19 ≤ <i>k</i> ≤ 19, −12 ≤ <i>l</i> ≤ 13
Number of measured reflections	16236	7407
Number of unique reflections	6087 (<i>R</i> _{int} = 0.0517)	2580 (<i>R</i> _{int} = 0.0223)
Number of reflections with <i>I</i> > 2σ(<i>I</i>)	4129	2273
Number of refinement variables	427	184
<i>R</i> Factors based	<i>R</i> ₁ = 0.1231, <i>wR</i> ₂ = 0.2619	<i>R</i> ₁ = 0.0272, <i>wR</i> ₂ = 0.0726
on reflections with <i>I</i> > 2σ(<i>I</i>)	<i>R</i> ₁ = 0.1691, <i>wR</i> ₂ = 0.2865	<i>R</i> ₁ = 0.0336, <i>wR</i> ₂ = 0.0748
Goodness-of-fit on <i>F</i> ²	1.084	1.043
Residual electron density (min/max) / e Å ⁻³	−1.018/1.849	−0.443/0.416

The complexation of crown (*E*)-**1** with ammonium compound (*E*)-**4** in MeCN was studied using two procedures.

Method I. Absorption spectra of mixtures of (*E*)-**1** and (*E*)-**4** were measured in the range of 395–500 nm at a fixed total concentration of (*E*)-**1** ($C_A = 2.8 \cdot 10^{-5}$ mol L⁻¹, 10 mm cuvette) and at different total concentrations of (*E*)-**4** ($C_B = (0-6) \cdot 10^{-4}$ mol L⁻¹). The ionic strength of the solution (*I*_S) was maintained at 0.01 mol L⁻¹ using the supporting electrolyte Bu₄NClO₄. The stability constant of the complex (*E*)-**1**·(*E*)-**4** was determined by the parameterized matrix modeling of spectroscopic data.²⁵

Method II. Absorption spectra of equimolar mixtures of (*E*)-**1** and (*E*)-**4** were measured in the range of 220–500 nm at different concentrations of the components ($C_A = C_B = 1 \cdot 10^{-5}$ – $3.6 \cdot 10^{-4}$ mol L⁻¹) in cuvettes with different optical path lengths. The initial mixture ($C_A = C_B = 3.6 \cdot 10^{-4}$ mol L⁻¹) was prepared by dissolving a weighed sample of the complex (*E*)-**1**·(*E*)-**4** in acetonitrile containing Bu₄NClO₄ at a concentration of 0.007 mol L⁻¹. Dilute solutions were prepared by the addition of the initial solution into MeCN containing Bu₄NClO₄ at a concentration of 0.01 mol L⁻¹. The precise values of *C*_A and *C*_B were determined from the optical density of the solution at 386 nm, where the sum of the extinction coefficients of the components is equal to the extinction coefficient of the complex. The position of the isosbestic point was determined in advance by comparing the spectra of an equimolar mixture of (*E*)-**1** and (*E*)-**4** before and after the addition of a weighed sample of the supporting electrolyte (upon the addition of the supporting electrolyte, the equilibrium was shifted toward the complex due

to an increase in the ionic strength of the solution). The absorption spectrum and the stability constant of the complex (*E*)-**1**·(*E*)-**4** at *I*_S = 0.01 mol L⁻¹ were obtained by the parameterized modeling of the spectroscopic data. In order to take into account small variations in the ionic strength of the solution, the modeling was performed using the activity coefficients of charged particles, which were calculated in the second approximation of the Debye–Hückel theory. The calculation procedure is described in detail in the Results and Discussion section.

In order to evaluate the quantum yield of the cross [2+2] PCA reaction between the molecules in the complex (*E*)-**1**·(*E*)-**4**, a solution of an equimolar mixture of compounds (*E*)-**1** and (*E*)-**4** ($C_A = C_B = 1 \cdot 10^{-4}$ mol L⁻¹, 2 mm cuvette) in the presence of Bu₄NClO₄ (0.01 mol L⁻¹) was irradiated at λ = 366 nm with the intensity *I*_{act} = 2.4 · 10⁻⁹ mol cm⁻² s⁻¹ for 35 min. The effective quantum yield was calculated by the equation

$$\Phi_{\text{PCA}} = (\Delta CD_0) / \{10^3 I_{\text{act}} t_{\text{ir}} \epsilon_{\text{AB}} [\text{AB}] (1 - 10^{-D})\},$$

$$D = (D_0 + D_{\text{ir}}) / 2,$$

where Δ*C* is the total consumption of **1** and **4** during the photolysis, *t*_{ir}; *D*₀ and *D*_{ir} are the optical densities of the solution at the irradiation wavelength before and after the photolysis, respectively; [AB] is the equilibrium concentration of the complex (*E*)-**1**·(*E*)-**4** before the photolysis; ε_{AB} is the extinction coefficient of (*E*)-**1**·(*E*)-**4** at the irradiation wavelength. The value of Δ*C* was measured using the following non-standard procedure.

Water (20 vol.%) was added to the photolysate solution, resulting in the complete dissociation of the complexes. This solution was irradiated at $\lambda = 366$ nm until the *E*–*Z*-photostationary state for unreacted compounds **1** and **4** was reached (the cycloadduct did not absorb light at $\lambda > 350$ nm). The same operations were performed for the control solution of an equimolar mixture of compounds (*E*)-**1** and (*E*)-**4**. The total consumption of compounds **1** and **4** in the [2+2] PCA reaction in the former solution was determined by comparing the absorption spectra of the photostationary states in two solutions (at $\lambda > 350$ nm).

Quantum chemical calculations. The conformations of the complex (*E*)-**1**·(*E*)-**4** in the gas phase were analyzed by the parameterized quantum chemical method, which was developed by D. N. Laikov²⁶ and implemented in the Priroda 14 program.²⁷ The calculations were performed for conformers of two principal types. In the conformers of one type, the styrylpyridinium cations are arranged one above another, whereas in the conformers of another type the cations are far apart. The most stable structures were selected based on the electronic energy, *i.e.*, without taking into account the zero-point vibrational energy and thermal corrections. The geometric parameters of two most stable conformers of the first type and one most stable conformer of the second type were optimized by the density functional theory method using the hybrid functional M06-2X (see Ref. 28) and the 6-31G(d) basis set. The solvent effects were taken into account in terms of the SMD continuum solvation model.²⁹ The calculations by the M06-2X/6-31G(d)/SMD method were performed with the Gaussian 09 program.³⁰

The effective diameters of cation (*E*)-**1**, dication (*E*)-**4**, and trication (*E*)-**1**·(*E*)-**4** required for the evaluation of the activity coefficients were calculated from the corresponding molecular volumes (using the formula for the ball diameter). The molecular volumes were calculated by the M06-2X/6-31G(d)/SMD method using the keyword "volume" and the internal command `iop(6/44 = 4)` activating the numerical integration of the density.

Results and Discussion

Synthesis and X-ray diffraction study. Ammonium compound **4** was prepared by fusing neutral 4-[(*E*)-2-(3,4-dichlorophenyl)vinyl]pyridine with 3-bromo-1-propylammonium bromide followed by the exchange of bromide anions with perchlorate ions by the treatment with concentrated perchloric acid in aqueous ethanol (see Scheme 2). Compound **4** was isolated as the *trans* isomer, as evidenced from the spin-spin coupling constant for ethylenic protons $^3J_{trans-CH=CH} = 16.4$ Hz.

The complex (*E*)-**1**·(*E*)-**4** was obtained in high yield by the crystallization of an equimolar mixture of the components from the benzene–acetonitrile solution. The stoichiometry of the complex (1 : 1) was determined based on the comparison of the integrated intensities of the corresponding signals in the ¹H NMR spectrum (in DMSO-*d*₆) and was confirmed by elemental analysis.

Compound **4** and model propane-1,3-diammonium diperchlorate were obtained as single crystals and were studied by X-ray diffraction. The structures of these compounds are shown in Fig. 1.

The structure of compound **4** was determined with low accuracy due apparently to the disorder of all structural units in the asymmetric unit of the crystal. Thus, both perchlorate anions are disordered over two positions characterized by the rotation about the center of mass for Cl(1)O₄ and the rocking along the line connecting the O(21) and O(22) atoms for Cl(2)O₄. The occupancy ratios for the disordered anions are 0.78 : 0.22 and 0.55 : 0.45, respectively. In addition, numerous residual electron density peaks are observed in the difference Fourier map around the Cl(2) and Cl(2') atoms, which are indicative of the presence of other positions of this anion with low occupancies. However, attempts to interpret these peaks as oxygen atoms failed.

The organic dication in structure **4** is disordered over two *s* conformations, which differ in the orientation of the ethylenic bond with respect to the dichlorobenzene moiety. The occupancy ratio for the conformers is 0.54 : 0.46. This is an example of the typical behavior of di(aryl/hetaryl)ethylenes in the crystals referred to as the temperature-dependent bicycle-pedal isomerization,^{31,32} which corresponds to the rotation of the ethylene group by 180° around single bonds with the retention of the *E* configuration of the double bond. Earlier,^{7,19,33} we have observed the bicycle-pedal isomerization of styryl dyes and neutral styryl heterocycles in a number of investigations of their crystal structures.

In the crystals of **4** and H₃N⁺(CH₂)₃NH₃⁺·2 ClO₄[−], the ammonium groups are surrounded by independent anions and their symmetrical equivalents in such a way that they form numerous bifurcated hydrogen bonds (see Fig. 1). The N⁺H···O distances are in the range of 2.09–2.58 Å. The angles at the hydrogen atoms vary in the range of 115–168°. These parameters characterize a relatively weak hydrogen bond and provide indirect evidence of the disorder of the perchlorate anions in structure **4**.

The chromophoric moiety of compound **4** is nearly planar in both *s* conformers. Thus, the dihedral angle between the planes of the pyridine and benzene rings is 7.5 and 8.7° for the major and minor conformers, respectively. This is indicative of the conjugation over the chromophore, although the C=C double bond is rather localized (the length of this bond in two conformers is 1.326(12) and 1.309(16) Å) compared to the adjacent formally single bonds (1.460(30)–1.497(16) Å). These geometric parameters are typical of styryl dyes of the 4-pyridine series.¹⁹

The characteristic feature of *N*-alkyl derivatives of pyridine is the almost perpendicular orientation of the alkyl substituent with respect to the plane of the pyridine ring, thus diminishing the steric interaction between atoms of the pyridine ring and its substituent. The same situation is observed in the crystal structure of **4**, in which the C_(Ar)–N(1)–C_(Alk)–C_(Alk) torsion angle is *ca.* 85°. It should be noted that the ammoniopropyl substituent in the crystal adopts a *trans,gauche* conformation, although the completely *transoid* conformation of this substituent should be

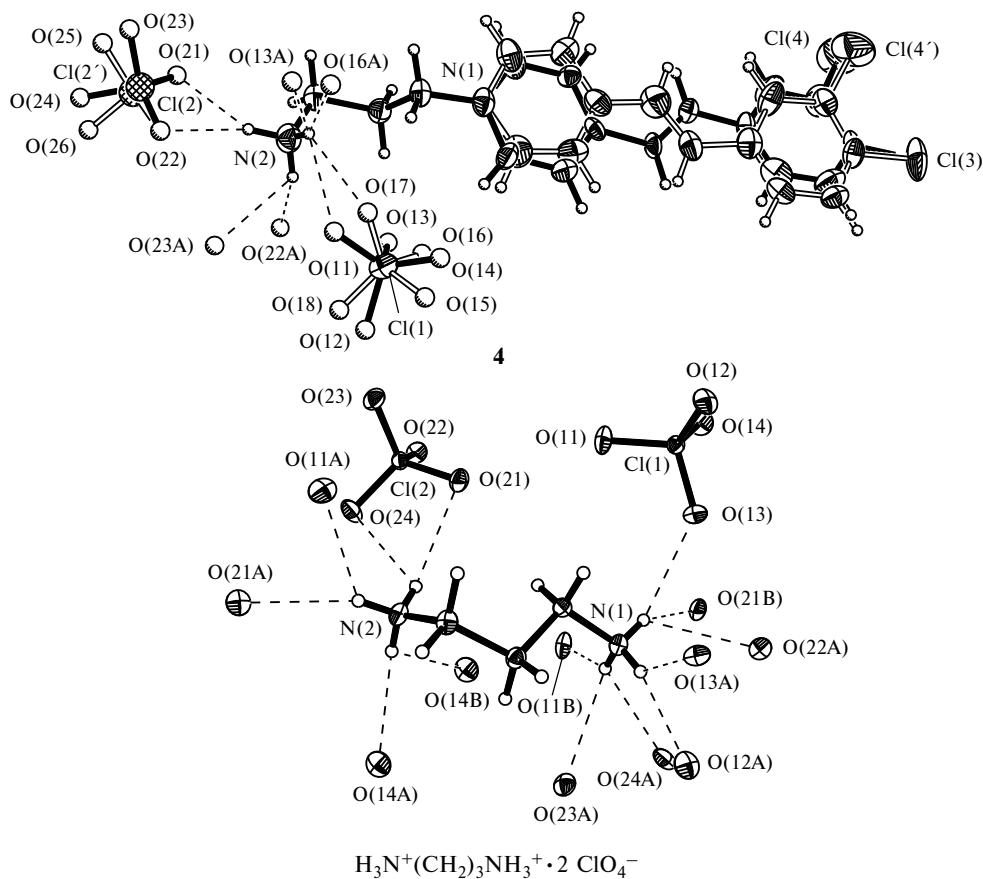


Fig. 1. Structures of compound **4** and propane-1,3-diammonium diperchlorate. The displacement ellipsoids are drawn at the 50% probability level. The additional letters A and B refer to symmetry-generated atoms. The hydrogen bonds are indicated by dashed lines. The minor components of the disordered moieties in compound **4** are shown as open lines.

most favorable (to minimize steric and Coulomb interactions). As shown below by molecular simulation methods, the *trans,gauche* conformation of the $\text{N}^+(\text{CH}_2)_3\text{NH}_3^+$ moiety is necessary for the conjugated moieties of compounds (*E*)-**1** and (*E*)-**4** to be brought into close proximity in the complex. It should be noted that the model compound $\text{H}_3\text{N}^+(\text{CH}_2)_3\text{NH}_3^+ \cdot 2\text{ClO}_4^-$ also adopts a *trans,gauche* conformation in the crystal. Many other

N-ammoniopropylpyridine derivatives studied earlier^{13,16,34} have this conformation in the crystals.

Photochemical properties of (*E*)-1** and (*E*)-**4**.** The absorption and fluorescence spectra of compound (*E*)-**4** in MeCN are shown in Fig. 2. Principal photochemical characteristics of (*E*)-**4**, crown compound (*E*)-**1**, and the complex (*E*)-**1** · $\text{H}_3\text{N}^+(\text{CH}_2)_3\text{NH}_3^+$ (see Ref. 17) are given in Table 2.

Table 2. Principal photochemical characteristics of compounds (*E*)-**4** and (*E*)-**1** and the complex (*E*)-**1** · $\text{H}_3\text{N}^+(\text{CH}_2)_3\text{NH}_3^+$ in MeCN^a

Compound	λ_{abs}	λ_{fl}	$\Delta E_{\text{S}}/\text{cm}^{-1}$	ϕ_{f}	$\tau_{\text{f}}/\text{ns}$	ϕ_{E-Z}	ϕ_{Z-E}
	nm						
(<i>E</i>)- 4	346	441	6200	0.004	<0.05	0.48	0.34
(<i>E</i>)- 1	399	560	7200	0.100	0.26/0.72 ^b	0.17	0.50
(<i>E</i>)- 1 · $\text{H}_3\text{N}^+(\text{CH}_2)_3\text{NH}_3^+$	384	543	7600	0.080	0.20/0.51 ^b	0.39	0.44

^a λ_{abs} is the position of the long-wavelength maximum in the absorption spectrum, λ_{fl} is the position of the maximum in the corrected fluorescence spectrum, ΔE_{S} is the Stokes shift, ϕ_{f} is the fluorescence quantum yield, τ_{f} is the fluorescence lifetime, ϕ_{E-Z} and ϕ_{Z-E} are the quantum yields of the forward and reverse *E*–*Z*-photoisomerization reactions, respectively.

^b Two-component decay.

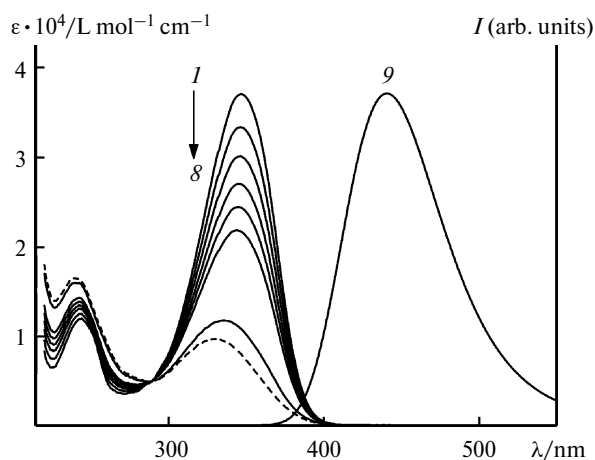


Fig. 2. Absorption spectra of compound (*E*)-4 before (1) and after the photolysis at $\lambda = 366$ nm for 8 (2), 16 (3), 24 (4), 32 (5), and 42 s (6) (the light intensity is $1 \cdot 10^{-9}$ mol cm^{-2} s^{-1}); the absorption spectrum of the *E*-*Z*-photostationary state (7); the absorption spectrum of compound (*Z*)-4 (8); the corrected fluorescence spectrum (*E*)-4 (9); MeCN as the solvent.

The spectroscopic and photochemical properties of compound (*E*)-4 are very similar to those of 1-alkyl-4-[2-(*E*)-(4-*R*-phenyl)vinyl]pyridinium salts ($R = \text{CN}, \text{H},$ or Me), which exhibit high quantum yields of *E*-*Z*-photoisomerization (0.4–0.5) and low fluorescence yields ($\varphi_f < 0.01$) in polar solvents.³⁵

Styryl dye (*E*)-1 is characterized by a relatively high fluorescence yield and a low quantum yield of the forward *E*-*Z*-photoisomerization. Figure 3 presents the data on the fluorescence kinetics of compound (*E*)-1. The kinetic curves at three different wavelengths correspond to the biexponential decay model with $\tau_1 = 0.26$ ns and $\tau_2 = 0.72$ ns

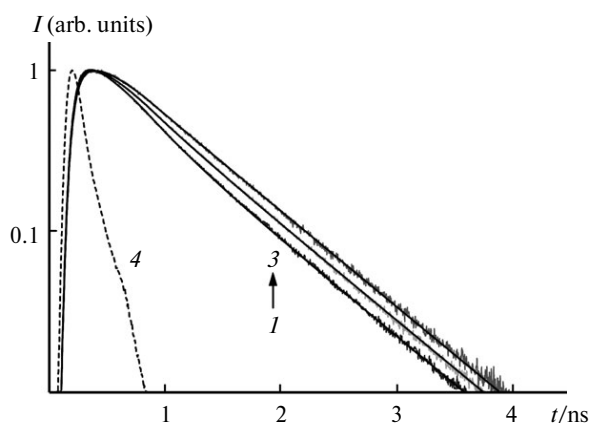
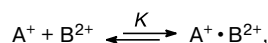


Fig. 3. Kinetic data on the fluorescence of dye (*E*)-1 in MeCN under 75-ps laser pulse excitation at $\lambda = 375$ nm and the observation at 510 (1), 560 (2), and 610 (3) nm; the laser pulse profile; the smooth curves are generated by the global fitting in terms of the biexponential decay model with $\tau_1 = 0.26$ ns and $\tau_2 = 0.72$ ns.

(the relative amplitudes of the fast component are 71, 31, and 2.5% at 510, 560, and 610 nm, respectively). Earlier, the two-component fluorescence decay has been observed for the 15-crown-5 analog of (*E*)-1.³⁶

The complexation of compound (*E*)-1 with $\text{H}_3\text{N}^+(\text{CH}_2)_3\text{NH}_3^+$ ions led to a considerable increase in φ_{E-Z} (more than twofold), a 20% decrease in φ_f , a 20–30% decrease in τ_1 and τ_2 , and an increase in the relative amplitude of the fast component of the fluorescence decay. The observed changes in the properties suggest that the slow component of the fluorescence decay in the case of (*E*)-1 may be associated with the transition of the excited dye molecule to the so-called twisted intramolecular charge transfer state (TICT state).³⁷ The co-existence of the *s-cis* and *s-trans* conformers of (*E*)-1 (see Fig. 1), one of which is characterized by the relatively high barrier for *E*-*Z*-photoisomerization, can be considered as an alternative explanation.

Complexation between (*E*)-1 and (*E*)-4. Figure 4 shows the results of spectrophotometric titration (SPT) of receptor (*E*)-1 with substrate (*E*)-4 in MeCN at an ionic strength of the solution $I_S = 0.01$ mol L^{-1} . The observed changes in the spectra were well reproduced by the parameterized matrix modeling²⁵ in terms of the simplest complexation model



where A^+ is cation (*E*)-1, B^{2+} is dication (*E*)-4, and K is the stability constant of the complex (L mol^{-1}). The determined stability constant ($\log K = 3.89$) appeared to be very similar to that of the complex (*E*)-1 \cdot $\text{H}_3\text{N}^+(\text{CH}_2)_3\text{NH}_3^+$ ($\log K = 3.97$ at an ionic strength of the solution of ca. 0.02 mol L^{-1} ; see Ref. 17).

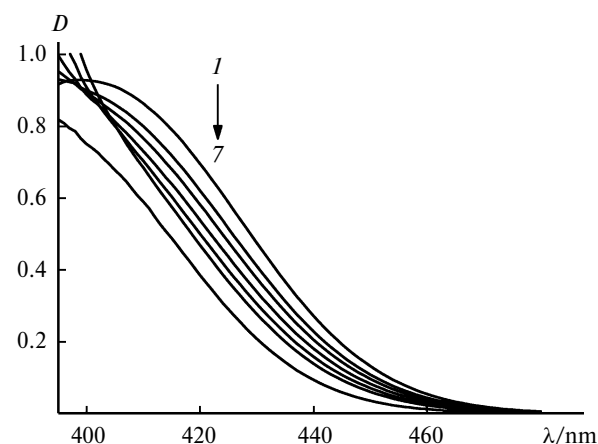


Fig. 4. Absorption spectra of mixtures of compounds (*E*)-1 and (*E*)-4 in MeCN (the ionic strength of the solution is 0.01 mol L^{-1}) at a fixed concentration of (*E*)-1 ($C_A = 2.8 \cdot 10^{-5}$ mol L^{-1}) and at different concentrations of (*E*)-4, mol L^{-1} : $C_B = 0$ (1), $7.3 \cdot 10^{-5}$ (2), $1.2 \cdot 10^{-4}$ (3), $2.2 \cdot 10^{-4}$ (4), $3.6 \cdot 10^{-4}$ (5), and $6.0 \cdot 10^{-4}$ (6). Curve 7, the calculated spectrum of the complex (*E*)-1 \cdot (*E*)-4.

The calculated absorption spectrum of the complex (*E*)-**1**·(*E*)-**4** is displayed in Fig. 4. The observed differences in the spectra of compounds (*E*)-**1** and (*E*)-**1**·(*E*)-**4** are attributed mainly to the hypsochromic shift of the absorption band of (*E*)-**1** due to the coordination of the ammoniopropyl group of (*E*)-**4** to the crown moiety of (*E*)-**1**. The cation-induced hypsochromic effects are characteristic of donor-acceptor chromoionophores of type (*E*)-**1**.^{38,39}

As mentioned above, if the receptor and the substrate have similar absorption spectra, the conventional SPT method is inapplicable to measurements of the stability constant of the complex. Therefore, we tested another procedure (see the Experimental).

Figure 5 shows the absorption spectra of equimolar mixtures of (*E*)-**1** and (*E*)-**4** at different total concentrations of the components. The stability constant and the absorption spectrum of the complex (*E*)-**1**·(*E*)-**4** were obtained by the parameterized matrix modeling of the spectra of equimolar mixtures. The calculation procedure is considered below.

By applying the law of mass action and the material balance principle on the condition that $C_A = C_B$, we derived the equation for the calculation of the equilibrium concentration of the complex

$$[AB] = K(C_A - [AB])^2 a_A a_B a_{AB}^{-1},$$

where a_A , a_B , and a_{AB} are the activity coefficients for cations (*E*)-**1**, (*E*)-**4**, and (*E*)-**1**·(*E*)-**4**, respectively. The activity coefficients were determined in the second approximation of the Debye–Hückel equation:

$$\log a = -H_1 z^2 (I_S^{-0.5} + H_2 d)^{-1},$$

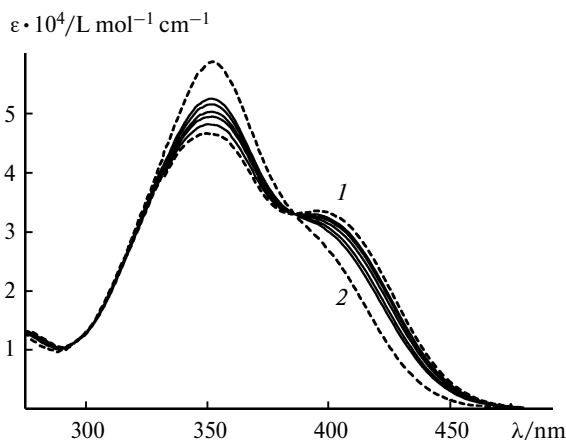


Fig. 5. Absorption spectra of equimolar mixtures of compounds (*E*)-**1** and (*E*)-**4** in MeCN at different total concentrations of the components (solid curves); the sum of the absorption spectra of compounds (*E*)-**1** and (*E*)-**4** (1) and the calculated spectrum of the complex (*E*)-**1**·(*E*)-**4** (2).

$$H_1 = 1.824 \cdot 10^6 (\mu T)^{-1.5},$$

$$H_2 = 50.29 (\mu T)^{-0.5},$$

where z and d are the charge and diameter of the ion, respectively, and μ is the solvent permittivity. For MeCN, $\mu = 35.85$ at $T = 298$ K;⁴⁰ consequently, $H_1 = 1.65$ and $H_2 = 0.49$. The effective diameters of cations (*E*)-**1**, (*E*)-**4**, and (*E*)-**1**·(*E*)-**4**, which were evaluated by quantum chemical modeling, are 10.2, 8.8, and 12.0 Å, respectively. The ionic strength of the solution for this system $I_S = 2[AB] + 4C_A + C_{SE}$, where C_{SE} is the concentration of the supporting electrolyte (Bu_4NClO_4).

According to the light absorption law, the spectrum of an equimolar mixture of (*E*)-**1** and (*E*)-**4** can be described by the equation $D(\lambda) = \epsilon_{AB}(\lambda)[AB]l + (\epsilon_A(\lambda) + \epsilon_B(\lambda)) \cdot (C_A - [AB])l$. The spectra measured at m different values of C_A can be represented as the matrix $\mathbf{D} = \mathbf{E}\mathbf{C}$ of the dimension $n \times m$, where n is the number of values of the optical density in the spectrum. The first column of the extinction coefficient matrix \mathbf{E} contains n values of $\epsilon_{AB}(\lambda)$; the second column, n values of $\epsilon_A(\lambda) + \epsilon_B(\lambda)$. The first row of the concentration matrix \mathbf{C} includes m values of $[AB]l$; the second row, m values of $(C_A - [AB])l$.

The parameterized modeling procedure of the matrix \mathbf{D} is as follows. First, the value of the constant K is postulated, and the concentrations $[AB]$ and $C_A - [AB]$ are determined by the numerical solution of Eq. (1). These concentrations compose the matrix \mathbf{C} . Then the theoretical extinction coefficient matrix $\mathbf{E}_{\text{cal}} = \mathbf{D}\mathbf{C}^T(\mathbf{C}\mathbf{C}^T)^{-1}$, where \mathbf{C}^T is the transpose of the matrix \mathbf{C} , and the theoretical matrix of spectra $\mathbf{D}_{\text{cal}} = \mathbf{E}_{\text{cal}}\mathbf{C}$ are calculated. The stability constant, the absorption spectrum of the complex, and the sum of the spectra of individual components are obtained simultaneously by the minimization of the standard deviation $\sigma(K)$ between \mathbf{D}_{cal} and the experimental matrix \mathbf{D} :

$$\sigma(K) = \sqrt{\frac{\sum_{i=1}^n \sum_{j=1}^m (D_{\text{cal}}^{ij} - D^{ij})^2}{nm}}.$$

The parameterized modeling was performed with the MATLAB program⁴¹ using the `fminbnd` function for the numerical solution of Eq. (1) and the `fminsearch` function for the minimization of $\sigma(K)$.

The stability constant of the complex (*E*)-**1**·(*E*)-**4** calculated by this method ($\log K = 3.87$ at $I_S = 0.01$ mol L⁻¹) is consistent with the constant measured by the SPT method. In the compatible region, the calculated spectrum of (*E*)-**1**·(*E*)-**4** (see Fig. 5) virtually coincides with the spectrum obtained from the SPT data.

[2+2] Photocycloaddition. Figure 6 shows the kinetics of the absorption spectra upon stationary photolysis of an equimolar mixture of compounds (*E*)-**1** and (*E*)-**4** in MeCN at $\lambda = 366$ nm. In the beginning of the process,

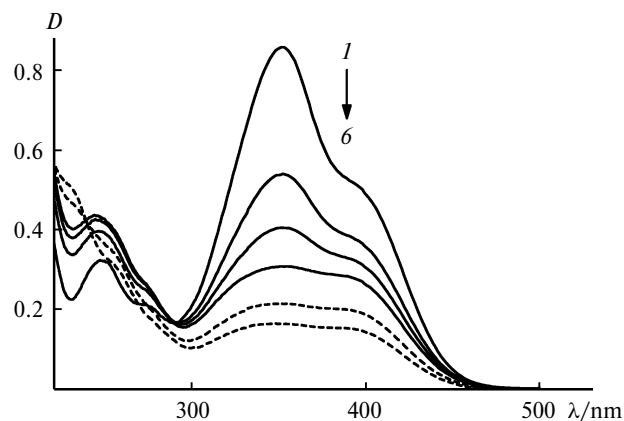


Fig. 6. Stationary photolysis of an equimolar mixture of compounds (*E*)-**1** and (*E*)-**4** in MeCN ($C_A = C_B = 3.3 \cdot 10^{-4} \text{ mol L}^{-1}$, 0.5 mm cuvette) at $\lambda = 366 \text{ nm}$ (the intensity is *ca.* $2 \cdot 10^{-9} \text{ mol cm}^{-2} \text{ s}^{-1}$). The time of photolysis is 0 (**1**), 1 (**2**), 2 (**3**), 7 (**4**), ~120 (**5**), and ~240 min (**6**).

rapid changes in the spectra associated with the *E*–*Z* photoisomerization of the components are observed. Then very slow changes take place, which are indicative of the consumption of compounds **1** and **4** in the [2+2] PCA reaction. Conceivably, the cycloaddition occurs between the molecules in the complex (*E*)-**1**·(*E*)-**4** (by analogy with the complex (*E*)-**1**·(*E*)-**2**; see Ref. 15). In the case of compounds (*E*)-**1** and (*E*)-**4**, the synthesis of the cross-photocycloadduct (analogous to *rectt*-**3**) in preparative amounts presented problems because of the low quantum

yield of PCA, which did not allow us to determine the structure of the cycloadduct. The effective quantum yield of [2+2] PCA in the complex (*E*)-**1**·(*E*)-**4** was evaluated by the procedure described in the Experimental section. The value of Φ_{PCA} was *ca.* 0.0018.

Molecular simulation. Figure 7 presents the geometry of three conformers of the complex (*E*)-**1**·(*E*)-**4** optimized by the M06-2X/6-31G(d)/SMD method. The relative electronic energies of these structures in MeCN and in the gas phase are given in Table 3 (the gas-phase energies were calculated by the method developed by D. N. Laikov).

According to the calculations, conformers, in which the chromophoric moieties are arranged one above another, are most stable in a polar solvent. This indicates that the dispersion attractive forces between the styrylpyridinium cations are stronger than the Coulomb repulsive forces. The conformer **C-a** with the *anti* arrangement of the Het–CH=CH–Ar groups is slightly more favorable than the *syn* conformer **C-b**. However, the energy difference is within the calculation error. Most likely, the *syn* and *anti* conformers co-exist in solution in comparable amounts. In the gas phase, the chromophoric moieties in the complex (*E*)-**1**·(*E*)-**4** are remote from each other due to stronger Coulomb repulsion.

In the structures **C-a** and **C-b**, the ammonium groups form directional hydrogen bonds with three crown oxygen atoms. The distances from these atoms to the ammonium nitrogen atom vary in the range of 2.81–2.91 Å. The calculated distances correspond to the crystallographic data published for the complexes of bis(18-crown-6)stilbene

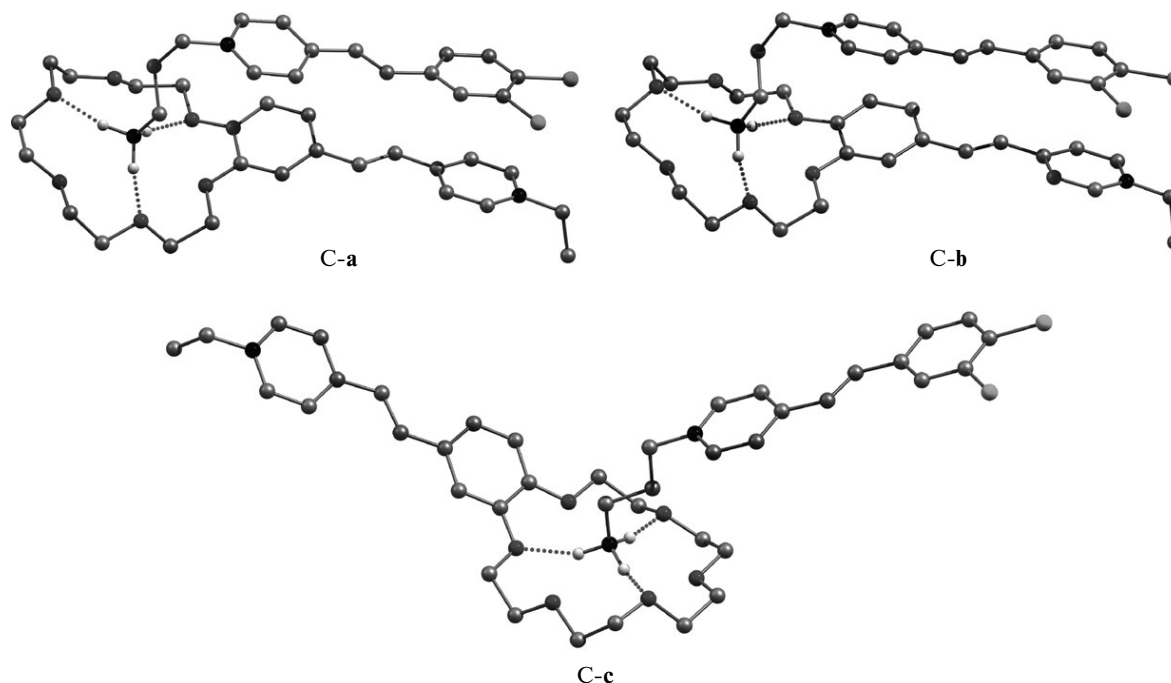


Fig. 7. Geometry of selected isomers of the complex (*E*)-**1**·(*E*)-**4** optimized by the M06-2X/6-31G(d)/SMD method (the hydrogen atoms are not shown except for the hydrogen atoms of the ammonium groups).

Table 3. Relative electronic energies of the conformers of the complex (E)-1•(E)-4

Conformer	$E_{\text{rel}}/\text{kcal mol}^{-1}$	
	MeCN ^a	Gas phase ^b
C-a	0	0
C-b	+0.3	+0.1
C-c	+8.9	-4.7

^a M06-2X/6-31G(d)/SMD.^b The parameterized quantum chemical method developed by D. N. Laikov.

with bis-ammonioalkyl derivatives of 4,4'-bipyridyl³⁴ and the salt $\text{H}_3\text{N}^+(\text{CH}_2)_3\text{NH}_3^+ \cdot 2\text{ClO}_4^-$ (see Ref. 42).

The distances between the midpoints of the C=C double bonds in the conformers C-a and C-b are $\sim 3.5 \text{ \AA}$, and the angles between the double bonds are *ca.* 75 and 17°, respectively. Based on the topochemical criteria,^{7,43,44} it can be predicted that the cross [2+2] PCA in the conformer C-a is unlikely to occur, whereas this reaction in the conformer C-b is quite possible.

To summarize, we synthesized a new ammoniopropyl derivative of 4-styrylpyridine (E)-4 and studied its crystal structure. Electronic spectroscopy studies and quantum chemical calculations showed that compound (E)-4 and crown-containing styryl dye (E)-1 in MeCN form a pseudodimeric complex, in which the styrylpyridinium cations are arranged one above another due to stacking interactions. The complex (E)-1•(E)-4 was also isolated in the pure state by the co-crystallization of the components. A procedure is proposed for the global analysis of the spectrophotometric data, which takes into account the effect of the ionic strength of the solution on the observed equilibrium reaction giving a complex. The evaluated stability constant of the complex (E)-1•(E)-4 ($\log K = 3.89$ at an ionic strength of 0.01 mol L^{-1}) is very similar to that of the complex (E)-1• $\text{H}_3\text{N}^+(\text{CH}_2)_3\text{NH}_3^+$ ($\log K = 3.97$). It was found that the complexation between compounds (E)-4 and (E)-1 activates the [2+2] photocycloaddition; however, the latter proceeds in low quantum yield (<0.002) due apparently to the electron-withdrawing effect of the chlorine atoms at positions 3 and 4 of the styryl moiety of (E)-4. Further studies are necessary in order to understand the low efficiency of the supramolecular photoreaction.

This study was financially supported by the Russian Science Foundation (Project No. 14-13-00076) and the Russian Academy of Sciences.

References

- J. Svoboda, B. König, *Chem. Rev.*, 2006, **106**, 5413.
- B. Bibal, C. Mongin, D. M. Bassani, *Chem. Soc. Rev.*, 2014, **43**, 4179.
- S. P. Gromov, *Russ. Chem. Bull. (Int. Ed.)*, 2008, **57**, 1325 [*Izv. Akad. Nauk, Ser. Khim.*, 2008, 1299].
- N. J. Turro, V. Ramamurthy, J. C. Scaiano, in *Modern Molecular Photochemistry of Organic Molecules*, University Science Books, Sausalito, 2010, Ch. 13, p. 925.
- Supramolecular Photochemistry: Controlling Photochemical Processes*, Eds V. Ramamurthy, Y. Inoue, Wiley, Hoboken, 2011, 640 pp.
- L. R. MacGillivray, G. S. Papaefstathiou, T. Frišćić, T. D. Hamilton, D.-K. Bučar, Q. Chu, D. B. Varshney, I. G. Georgiev, *Acc. Chem. Res.*, 2008, **41**, 280.
- L. G. Kuz'mina, A. I. Vedernikov, A. V. Churakov, E. Kh. Lermontova, J. A. K. Howard, M. V. Alfimov, S. P. Gromov, *CrystEngComm*, 2014, **16**, 5364.
- M. V. Alfimov, S. P. Gromov, O. B. Stanislavskii, E. N. Ushakov, O. A. Fedorova, *Russ. Chem. Bull. (Int. Ed.)*, 1993, **42**, 1385 [*Izv. Akad. Nauk, Ser. Khim.*, 1993, 1449].
- E. N. Ushakov, S. P. Gromov, A. V. Buevich, I. I. Baskin, O. A. Fedorova, A. I. Vedernikov, M. V. Alfimov, B. Eliasson, U. Edlund, *J. Chem. Soc., Perkin Trans. 2*, 1999, 601.
- S. P. Gromov, E. N. Ushakov, A. I. Vedernikov, N. A. Lobova, M. V. Alfimov, Yu. A. Strelenko, J. K. Whitesell, M. A. Fox, *Org. Lett.*, 1999, **1**, 1697.
- D. G. Amirsakis, A. M. Elizarov, M. A. Garcia-Garibay, P. T. Glink, J. F. Stoddart, A. J. P. White, D. J. Williams, *Angew. Chem., Int. Ed.*, 2003, **42**, 1126.
- S. P. Gromov, A. I. Vedernikov, E. N. Ushakov, N. A. Lobova, A. A. Botsmanova, L. G. Kuz'mina, A. V. Churakov, Yu. A. Strelenko, M. V. Alfimov, J. A. K. Howard, D. Johnels, U. G. Edlund, *New J. Chem.*, 2005, **29**, 881.
- S. P. Gromov, N. A. Lobova, A. I. Vedernikov, L. G. Kuz'mina, J. A. K. Howard, M. V. Alfimov, *Russ. Chem. Bull. (Int. Ed.)*, 2009, **58**, 1211 [*Izv. Akad. Nauk, Ser. Khim.*, 2009, 1179].
- S. P. Gromov, A. I. Vedernikov, L. G. Kuz'mina, N. A. Lobova, S. S. Basok, Yu. A. Strelenko, M. V. Alfimov, *Russ. Chem. Bull. (Int. Ed.)*, 2009, **58**, 108 [*Izv. Akad. Nauk, Ser. Khim.*, 2009, 108].
- A. I. Vedernikov, S. K. Sazonov, P. S. Loginov, N. A. Lobova, M. V. Alfimov, S. P. Gromov, *Mendeleev Commun.*, 2007, **17**, 29.
- A. I. Vedernikov, S. K. Sazonov, L. G. Kuz'mina, J. A. K. Howard, M. V. Alfimov, S. P. Gromov, *Russ. Chem. Bull. (Int. Ed.)*, 2009, **58**, 1955 [*Izv. Akad. Nauk, Ser. Khim.*, 2009, 1893].
- A. I. Vedernikov, E. N. Ushakov, N. A. Lobova, A. A. Kiselev, M. V. Alfimov, S. P. Gromov, *Russ. Chem. Bull. (Int. Ed.)*, 2005, **54**, 666 [*Izv. Akad. Nauk, Ser. Khim.*, 2005, 656].
- A. I. Vedernikov, S. P. Gromov, N. A. Lobova, L. G. Kuz'mina, Yu. A. Strelenko, J. A. K. Howard, M. V. Alfimov, *Russ. Chem. Bull. (Int. Ed.)*, 2005, **54**, 1954 [*Izv. Akad. Nauk, Ser. Khim.*, 2005, 1896].
- A. I. Vedernikov, L. G. Kuz'mina, S. K. Sazonov, N. A. Lobova, P. S. Loginov, A. V. Churakov, Yu. A. Strelenko, J. A. K. Howard, M. V. Alfimov, S. P. Gromov, *Russ. Chem. Bull. (Int. Ed.)*, 2007, **56**, 1860 [*Izv. Akad. Nauk, Ser. Khim.*, 2007, 1797].
- SAINT, Version 6.02A*, Bruker AXS Inc., Madison, Wisconsin (USA), 2001.
- SHELXTL-Plus, Version 5.10*, Bruker AXS Inc., Madison, Wisconsin (USA), 1997.

22. K. Suzuki, A. Kobayashi, S. Kaneko, K. Takehira, T. Yoshihara, H. Ishida, Y. Shiina, S. Oishi, S. Tobita, *Phys. Chem. Chem. Phys.*, 2009, **11**, 9850.
23. E. N. Ushakov, V. A. Nadtochenko, S. P. Gromov, A. I. Vedernikov, N. A. Lobova, M. V. Alfimov, F. E. Gostev, A. N. Petrukhin, O. M. Sarkisov, *Chem. Phys.*, 2004, **298**, 251.
24. E. N. Ushakov, S. P. Gromov, L. G. Kuz'mina, A. I. Vedernikov, V. G. Avakyan, J. A. K. Howard, M. V. Alfimov, *Russ. Chem. Bull. (Int. Ed.)*, 2004, **53**, 1549 [*Izv. Akad. Nauk, Ser. Khim.*, 2004, 1491].
25. E. N. Ushakov, S. P. Gromov, O. A. Fedorova, Yu. V. Pershina, M. V. Alfimov, F. Barigelletti, L. Flamigni, V. Balzani, *J. Phys. Chem. A*, 1999, **103**, 11188.
26. D. N. Laikov, *J. Chem. Phys.*, 2011, **135**, 134120.
27. D. N. Laikov, *Priroda 14 (2014.02.23)*, *Quantum Chemical Program*, Lomonosov Moscow State University, Moscow (Russian Federation), 2014.
28. Y. Zhao, D. G. Truhlar, *Theor. Chem. Acc.*, 2008, **120**, 215.
29. A. V. Marenich, C. J. Cramer, D. G. Truhlar, *J. Phys. Chem. B*, 2009, **113**, 6378.
30. *Gaussian 09, Revision B.01*, Gaussian, Inc., Wallingford CT (USA), 2010.
31. J. Harada, K. Ogawa, *Chem. Soc. Rev.*, 2009, **38**, 2244.
32. E. Elacqua, P. Kaushik, R. H. Groeneman, J. C. Sumrak, D.-K. Bučar, L. R. MacGillivray, *Angew. Chem. Int. Ed.*, 2012, **51**, 1037.
33. L. G. Kuz'mina, A. I. Vedernikov, N. A. Lobova, S. K. Sazonov, S. S. Basok, J. A. K. Howard, S. P. Gromov, *Russ. Chem. Bull. (Int. Ed.)*, 2009, **58**, 1192 [*Izv. Akad. Nauk, Ser. Khim.*, 2009, 1161].
34. A. I. Vedernikov, E. N. Ushakov, A. A. Efremova, L. G. Kuz'mina, A. A. Moiseeva, N. A. Lobova, A. V. Churakov, Yu. A. Strelenko, M. V. Alfimov, J. A. K. Howard, S. P. Gromov, *J. Org. Chem.*, 2011, **76**, 6768.
35. H. Görner, A. Fojtik, J. Wróblewski, L. J. Currell, *Z. Naturforsch.*, 1985, **40a**, 525.
36. E. V. Tulyakova, O. A. Fedorova, Yu. V. Fedorov, G. Jonusauskas, A. V. Anisimov, *Russ. Chem. Bull. (Int. Ed.)*, 2007, **56**, 2166 [*Izv. Akad. Nauk, Ser. Khim.*, 2007, 2092].
37. Z. R. Grabowski, K. Rotkiewicz, W. Rettig, *Chem. Rev.*, 2003, **103**, 3899.
38. E. N. Ushakov, M. V. Alfimov, S. P. Gromov, *Russ. Chem. Rev.*, 2008, **77**, 39 [*Usp. Khim.*, 2008, **77**, 39].
39. E. N. Ushakov, M. V. Alfimov, S. P. Gromov, *Macroheterocycles*, 2010, **3**, 189.
40. J.-F. Côté, D. Brouillette, J. E. Desnoyers, J.-F. Rouleau, J.-F. St-Arnaud, G. Perron, *J. Solution Chem.*, 1996, **25**, 1163.
41. *MATLAB, Version 7.7, The Language of Technical Computing*, The MathWorks, Inc., Natick MA (USA), 2008.
42. S. P. Gromov, A. I. Vedernikov, N. A. Lobova, L. G. Kuz'mina, S. S. Basok, Yu. A. Strelenko, M. V. Alfimov, J. A. K. Howard, *New J. Chem.*, 2011, **35**, 724.
43. G. M. J. Schmidt, *Pure Appl. Chem.*, 1971, **27**, 647.
44. V. Ramamurthy, K. Venkatesan, *Chem. Rev.*, 1987, **87**, 433.

Received November 26, 2014